JOURNAL OF Applied Polymer SCIENCE

Special Issue: Bio-based Packaging

Guest Editors: José M. Lagarón, Amparo López-Rubio, and María José Fabra
Institute of Agrochemistry and Food Technology of the Spanish Council for Scientific Research

EDITORIAL

REVIEWS

RESEARCH ARTICLES

JOURNAL OF Applied Polymer SCIENCE

Special Issue: Bio-based Packaging

Guest Editors: José M. Lagarón, Amparo López-Rubio, and María José Fabra
Institute of Agrochemistry and Food Technology of the Spanish Council for Scientific Research

Impact of fermentation residues on the thermal, structural, and rheological properties of polyhydroxy(butyrate-*co*-valerate) produced from cheese whey and olive oil mill wastewater
L. Hilliou, D. Machado, C. S. S. Oliveira, A. R. Gouveia, M. A. M. Reis, S. Campanari, M. Villano and M. Majone, *J. Appl. Polym. Sci.* 2015, DOI: 10.1002/app.42818

Synergistic effect of lactic acid oligomers and laminar graphene sheets on the barrier properties of polylactide nanocomposites obtained by the in situ polymerization pre-incorporation method
J. Ambrosio-Martín, A. López-Rubio, M. J. Fabra, M. A. López-Manchado, A. Sorrentino, G. Gorrasi and J. M. Lagarón, *J. Appl. Polym. Sci.* 2015, DOI: 10.1002/app.42661

Antibacterial poly(lactic acid) (PLA) films grafted with electrospun PLA/allyl isothiocyanate fibers for food packaging
H. H. Kara, F. Xiao, M. Sarker, T. Z. Jin, A. M. M. Sousa, C.-K. Liu, P. M. Tomasula and L. Liu, *J. Appl. Polym. Sci.* 2015, DOI: 10.1002/app.42475

Poly(L-lactide)/ZnO nanocomposites as efficient UV-shielding coatings for packaging applications
E. Lizundia, L. Ruiz-Rubio, J. L. Vilas and L. M. León, *J. Appl. Polym. Sci.* 2015, DOI: 10.1002/app.42426

Effect of electron beam irradiation on the properties of polylactic acid/montmorillonite nanocomposites for food packaging applications
M. Salvatore, A. Marra, D. Duraccio, S. Shayanfar, S. D. Pillai, S. Cimmino and C. Silvestre, *J. Appl. Polym. Sci.* 2015, DOI: 10.1002/app.42219

Preparation and characterization of linear and star-shaped poly L-lactide blends
M. B. Khajeheian and A. Rosling, *J. Appl. Polym. Sci.* 2015, DOI: 10.1002/app.42231

Mechanical properties of biodegradable polylactide/poly(ether-block-amide)/thermoplastic starch blends: Effect of the crosslinking of starch
L. Zhou, G. Zhao and W. Jiang, *J. Appl. Polym. Sci.* 2015, DOI: 10.1002/app.42297

Interaction and quantification of thymol in active PLA-based materials containing natural fibers
I. S. M. A. Tawakkal, M. J. Cran and S. W. Bigger, *J. Appl. Polym. Sci.* 2015, DOI: 10.1002/app.42160

Graphene-modified poly(lactic acid) for packaging: Material formulation, processing, and performance
M. Barletta, M. Puopolo, V. Tagliaferri and S. Vesco, *J. Appl. Polym. Sci.* 2015, DOI: 10.1002/app.42252

Edible films based on chia flour: Development and characterization
M. Dick, C. H. Pagno, T. M. H. Costa, A. Gomaa, M. Subirade, A. De O. Rios and S. H. Flóres, *J. Appl. Polym. Sci.* 2015, DOI: 10.1002/app.42455

Influence of citric acid on the properties and stability of starch-polycaprolactone based films
R. Ortega-Toro, S. Collazo-Bigliardi, P. Talens and A. Chiralt, *J. Appl. Polym. Sci.* 2015, DOI: 10.1002/app.42220

Bionanocomposites based on polysaccharides and fibrous clays for packaging applications
A. C. S. Alcântara, M. Darder, P. Aranda, A. Ayral and E. Ruiz-Hitzky, *J. Appl. Polym. Sci.* 2015, DOI: 10.1002/app.42362

Hybrid carrageenan-based formulations for edible film preparation: Benchmarking with kappa carrageenan
F. D. S. Larotonda, M. D. Torres, M. P. Gonçalves, A. M. Sereno and L. Hilliou, *J. Appl. Polym. Sci.* 2015, DOI: 10.1002/app.42263

JOURNAL OF Applied Polymer SCIENCE

Special Issue: Bio-based Packaging

Guest Editors: José M. Lagarón, Amparo López-Rubio, and María José Fabra
Institute of Agrochemistry and Food Technology of the Spanish Council for Scientific Research

Structural and mechanical properties of clay nanocomposite foams based on cellulose for the food packaging industry
S. Ahmadzadeh, J. Keramat, A. Nasirpour, N. Hamdami, T. Behzad, L. Aranda, M. Vilasi and S. Desobry, *J. Appl. Polym. Sci.* 2015, DOI: 10.1002/app.42079

Mechanically strong nanocomposite films based on highly filled carboxymethyl cellulose with graphene oxide
M. El Achaby, N. El Miri, A. Snik, M. Zahouily, K. Abdelouahdi, A. Fihri, A. Barakat and A. Solhy, *J. Appl. Polym. Sci.* 2015, DOI: 10.1002/app.42356

Production and characterization of microfibrillated cellulose-reinforced thermoplastic starch composites
L. Lendvai, J. Karger-Kocsis, Á. Kmetty and S. X. Drakopoulos, *J. Appl. Polym. Sci.* 2015, DOI: 10.1002/app.42397

Development of bioplastics based on agricultural side-stream products: Film extrusion of *Crambe abyssinica*/wheat gluten blends for packaging purposes
H. Rasel, T. Johansson, M. Gällstedt, W. Newson, E. Johansson and M. Hedenqvist, *J. Appl. Polym. Sci.* 2015, DOI: 10.1002/app.42442

Influence of plasticizers on the mechanical and barrier properties of cast biopolymer films
V. Jost and C. Stramm, *J. Appl. Polym. Sci.* 2015, DOI: 10.1002/app.42513

The effect of oxidized ferulic acid on physicochemical properties of bitter vetch (*Vicia ervilia*) protein-based films
A. Arabestani, M. Kadivar, M. Shahedi, S. A. H. Goli and R. Porta, *J. Appl. Polym. Sci.* 2015, DOI: 10.1002/app.42894

Effect of hydrochloric acid on the properties of biodegradable packaging materials of carboxymethylcellulose/poly(vinyl alcohol) blends
M. D. H. Rashid, M. D. S. Rahaman, S. E. Kabir and M. A. Khan, *J. Appl. Polym. Sci.* 2015, DOI: 10.1002/app.42870

Journal of Applied Polymer Science

On the use of tris(nonylphenyl) phosphite as a chain extender in melt-blended poly(hydroxybutyrate-*co*-hydroxyvalerate)/clay nanocomposites: Morphology, thermal stability, and mechanical properties

Jennifer González-Ausejo, Estefania Sánchez-Safont, José Gámez-Pérez, Luis Cabedo
Polymer and Advanced Materials Group (PIMA), Universidad Jaume I, 12071 Castellon, Spain
Correspondence to: L. Cabedo (E-mail: lcabedo@uji.es)

ABSTRACT: The influence of the incorporation of tris(nonylphenyl) phosphite (TNPP) as a chain extender on the morphology and thermal stability of poly(hydroxybutyrate-*co*-hydroxyvalerate) (PHBV)/clay nanocomposites obtained by melt mixing has been studied. Two different clays have been used: a laminar organomodified montmorillonite (Cloisite® 30B) and a tubular unmodified halloysite (HNT). The morphology of the so-obtained nanocomposites has been assessed by transmission electron microscopy, scanning electron microscopy, and wide angle X-ray diffraction, showing a partially exfoliated structure for PHBV/Cloisite® 30B nanocomposites, as well as a good dispersion of the HNT in the PHBV matrix. The crystallinity of the resulting nanocomposites, determined by DSC, does not change when clays or TNPP are added. An increase in the onset temperature of thermal degradation of PHBV has been obtained with the addition of TNPP, as determined by TGA. With regard to the effect of the nanoclays on the thermal stability of PHBV, the onset temperature of the PHBV/HNT nanocomposites is higher than that of the pure PHBV, while this trend is not observed for the nanocomposites containing Cloisite® 30B. The addition of TNPP to the PHBV/Cloisite® 30B nanocomposites resulted in an improved thermal stability; however, for the HNT nanocomposites, the TNPP does not seem to have a significant effect. For all studied systems, it was shown that the variation of mechanical properties of the nanocomposites is due to the reinforcing effect of the nanoclays on the PHBV matrix. In the case of TNPP, it is due to the increased molecular weight and formation of a long-chain branching structure. © 2015 Wiley Periodicals, Inc. J. Appl. Polym. Sci. **2016**, *133*, 42390.

KEYWORDS: biopolymers and renewable polymers; clay; nanoparticles; nanowires and nanocrystals; thermogravimetric analysis

Received 13 February 2015; accepted 21 April 2015
DOI: 10.1002/app.42390

INTRODUCTION

Poly(hydroxybutyrate-*co*-hydroxyvalerate) (PHBV), a biodegradable copolyester from the polyhydroxyalkanoate (PHA) family, has gained a lot of attention because of its fast biodegradability and biocompatibility as well as a non-food-competitive origin.[1] Particularly in the packaging field, PHBV has shown a great interest because of its inertness and chemical stability that makes it suitable for applications as films for food contact material with any type of food.[2] It has been suggested that PHBV could replace polypropylene[3] or poly(ethylene terephtalate)[4] in many applications where it would not be necessary to modify their processing. In spite of the significant potential of PHBV to substitute commodity polymers, it still presents a number of property and processing shortcomings that hinder its use in many applications.[5] When compared to other linear polymers, PHBV has shown lower mechanical and gas barrier properties, as well as lower thermal resistance during processing.[4,6]

Nanotechnology brings significant opportunities to improve the applicability of PHBV to the food packaging field.[5,7] The increase in mechanical properties of biopolymers by incorporating low amounts of nanoparticles has been widely reported.[6,8,9] Indeed, some works have shown that the use of nanocomposites in food packaging applications, when properly prepared, is harmless and free potential migration issues.[7] The obtaining of polymer nanocomposites has been reported to be a promising way to improve the barrier properties against gases, aromas, and water vapor. Some reported nanofillers are carbon nanotubes, nanoclays, and halloysite nanotubes, among others.[6,10]

The montmorillonite is the most commonly used nanoclay in the field of polymer nanocomposites.[8] It is a natural clay belonging to the family of 2:1 layered silicates, also called 2:1 phyllosilicates. Its structure consists of layers made up of two tetrahedrally coordinated silicon atoms bonded to an edge-shared octahedral sheet of either aluminum or magnesium hydroxide. This nanoclay requires surface modification (organomodification) to achieve a good

degree of delamination when mixed with polymers. The chemicals more widely used for organomodification of montmorillonites are alkylammonium cations. In the case of PHBV nanocomposites, the use of organomodified clays containing surfactants appears to be a suitable way to improve their affinity to the polymer and dispersion within the matrix.[11–13] However, the addition of organomodified clays can lead to higher polymer degradation during melt processing,[11–13] due to a catalytic effect of their decomposition products.[13–15]

Recently, halloysite nanotubes (HNTs) have attracted interest as nanoparticles for biopolymers because they are economical and abundantly available and have rich functionality, good biocompatibility, and high mechanical strength.[16] Halloysite belongs to the kaolin group of clay minerals. It exhibits a predominantly hollow tubular structure in the nanoscale range and a large aspect ratio.[17]

As mentioned before, the degradation of biopolyesters, more specifically PHBV, during processing in molten conditions is a factor that inevitably limits the range of applications.[18] The use of chain extenders is a convenient approach for improving the thermal stability of biopolyesters during processing.[19–28] The chain extension is a reaction that avoids a drop in molecular weight. The reaction between carboxylic end groups on polyesters and the functional groups of chain extenders, such as hydroxyl, amine, anhydride, epoxy, or carboxylic acid, are the key reactions for improving thermal resistance.[29] This approach has been successfully applied to blends from several matrices.[19,20,25–27]

Some studies have developed the use of DCP[30,31] or Joncryl® ADR-4368[32] in PHBV. Haene *et al.*[30] studied the branching behavior of PHBV using low levels of DCP, reporting a branching process of PHBV observed from the increase in strain hardening with the addition of higher concentrations of DCP. Fei *et al.*[31] studied the cross-linking of PHBV using a high level of DCP and observed enhanced melt viscosity and mechanical properties without compromising the biodegradability. Duangphet *et al.*[32] studied the effect of an epoxy-functionalized chain extender (Joncryl® ADR-4368 S) on degradation during melt blending of PHBV conducted in a twin-screw extruder, showing an improvement in the resistance to thermal decomposition of PHBV, an enhancement of PHBV melt viscosity, and also a reduction of the crystallization rate by introducing the chain extender due to the increase in molecular weight and chain rigidity.

The use of chain extenders in the production of polymer-based nanocomposites has been studied.[19–21,23] According to Najafi *et al.*,[19–21] the incorporation of a chain extender into the nanocomposites had a profound effect on controlling the degradation and also increasing the molecular weight, resulting in an increase of the polymer viscosity.[19–21] Also, Meng *et al.*[23] found that the chain extenders have a remarkable stabilization effect on PLA/clay nanocomposites without negatively affecting the clay dispersion.[23]

Tris(nonylphenyl) phosphite (TNPP) has been successfully used as chain extender in other matrices[25–27] leading to thermal stabilization with low contents. Indeed, TNPP is characterized by being suitable for food contact,[33] thus being suitable for food packaging applications. However, to the best of our knowledge, its effect in PHBV has never been studied.

Within this context, the aim of this study was to evaluate the effect of the addition of TNPP as a chain extender with two types of clays (Cloisite® 30B and halloysite nanotubes) on the morphology, thermal, and mechanical properties of PHBV nanocomposites for food packaging applications.

EXPERIMENTAL

Materials

PHBV with 3 mol % hydroxyvalerate content was purchased from Tianan Biologic Material Co. (Ningbo, P.R. China) in pellet form (ENMAT Y1000P). Two different commercial nanoclays were used in this study: organomodified montmorillonite Cloisite® 30B (hereafter referred to as C30B) containing a methyl bis-2-hydroxyethyl ammonium quaternary salt, supplied by Southern Clay Products; and halloysite (HNT), an unmodified tubular clay from NaturalNano Inc. The chain extender used was tris(nonylphenyl) phosphite (TNNP) supplied by Sigma Aldrich.

Nanocomposite Preparation

PHBV and the clays used in this study were dried under vacuum at 80°C for 2 h before use, while the chain extender was used as received. The PHBV blends and nanocomposites were obtained by melt blending using an internal mixer (Rheomix 3000P ThermoHaake, Karlsruhe, Germany) during a mixing time of less than 6 min at a temperature of 180°C and rotor speed of 100 rpm. The mixer is provided with a software for displaying the variation of temperature (chamber and melt) and the torque during mixing. According to the record of the sensor of melt temperature during mixing, the melt temperature never reached 195°C, which guaranteed that there was no severe thermal degradation during blending. Plates (0.8 mm thick) and films (0.1 mm thick) were obtained from the blends by melting in a hot-plate press at 185°C and applying during 2 min for premelting followed by 3 bar for 3. Plates were used for morphological and thermal characterization, while films were used for the mechanical characterization. All the samples were stored in a vacuum desiccator at ambient temperature for 2 weeks to allow full crystallization to take place.[34–36]

Samples of both PHBV (referred to as neat PHBV) and PHBV with 1 wt % TNPP (PHBV–TNPP) were processed. The nomenclature used for the nanocomposites is as follows: PHBV-C30B and PHBV-HNT for the systems containing 5 wt % of Cloisite 30B and halloysite nanotubes, respectively, and PHBV–C30B–TNPP and PHBV–HNT–TNPP for the systems containing 5 wt % of Cloisite 30B and halloysite nanotubes together with 1 wt % TNPP as a chain extender.

Characterization

Transmission electron microscopy (TEM) of the nanocomposites was performed using a Jeol 2100 operated at 200 kV. The ultrathin sections with a thickness of 80 nm were prepared at room temperature using an RMC ultramicrotome (Model Powertome XL). The so-obtained films were placed on a carbon-coated copper grid for observation.

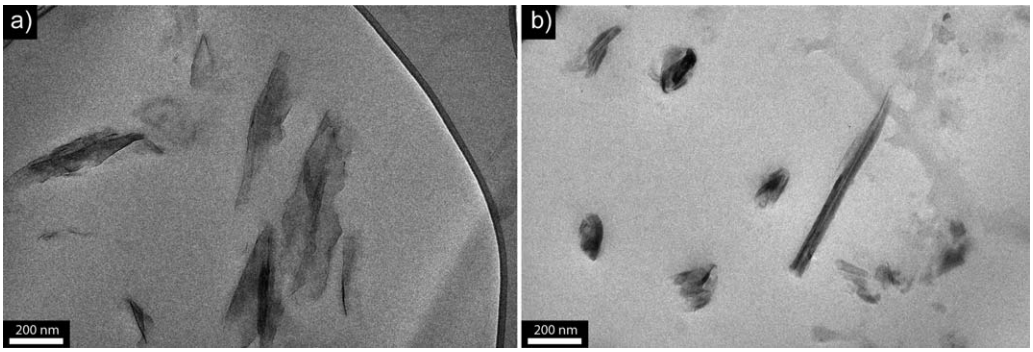

Figure 1. TEM micrograph of (a) PHBV–C30B and (b) PHBV–HNT.

The morphology of the cryofractured surface of PHBV nanocomposites was evaluated by scanning electron microscopy (SEM) using a JEOL 7001F. The samples were fractured in liquid nitrogen and subsequently coated by sputtering with a thin layer of Pt.

Wide-angle X-ray diffraction (WAXS) measurements were performed using a Bruker AXS D4 Endeavour diffractometer. The samples were scanned at room temperature in reflection mode using incident Cu Ka radiation ($k = 1.54$ Å), while the generator was set up at 40 kV and 40 mA. The data were collected over a range of scattering angles (2θ) of 2–30°. The basal spacing (d-spacing) of the clays was estimated from the (001) diffraction peak using Bragg's law, where λ is the wavelength of incident wave:

$$\lambda = 2 \cdot d \cdot \sin\theta \quad (1)$$

The thermal stability of the nanocomposites was investigated by means of thermogravimetric analysis (TGA) using a TG-STDA Mettler Toledo model TGA/SDTA851e/LF/1600. The samples were heated from 50 to 900°C at a heating rate of 10°C/min under nitrogen flow. The characteristic temperatures $T_{5\%}$ and T_d corresponded, respectively, to the initial decomposition temperature (5% of degradation) and to the maximum degradation rate temperature measured at the DTG peak maximum.

Differential scanning calorimeter (DSC) experiments were conducted using a PerkinElmer DSC-7. The weight of the DSC samples was typically 6 mg. Samples were first heated from 45 to 200°C at 40°C/min, kept for 1 min at 200°C, cooled down to 45°C at 10°C/min, and then finally heated to 200°C at 10°C/min. The crystallization temperature (T_c), melt temperature (T_m), and melting enthalpy (ΔH_m) were determined from the cooling and second heating curve. T_m and ΔH_m were taken as the peak temperature and the area of the melting endotherm, respectively. The crystallinity (X_c) of the PHBV phase was calculated by the following expression:

$$X_c(\%) = \frac{\Delta H_m}{w \cdot \Delta H_m^o} \cdot 100 \quad (2)$$

where ΔH_m (J/g) is the melting enthalpy of the polymer matrix, ΔH_m^0 is the melting enthalpy of 100% crystalline PHBV (perfect crystal) (146 J/g), and w is the polymer weight fraction of PHBV in the blend.[9] The DSC instrument was calibrated with an indium standard before use.

Tensile properties were measured in a universal testing machine (Instron 4469) at a cross-head speed of 10 mm/min and room temperature. All samples were conditioned under ambient conditions (25°C and 50% R.H. for 24 h). Tests were carried out according to ASTM D638 using films of approximately 100 μm thickness prepared by hot press. Five specimens of each sample were tested and the average results with standard deviation were reported.

RESULTS AND DISCUSSION

Morphology

The morphology of the PHBV nanocomposites was evaluated by means of SEM, TEM, and WAXS. Figure 1(a,b) presents the TEM micrographs of the PHBV nanocomposites with 5 wt % of C30B and HNT, respectively.

The effect of nanoclays on the properties of the polymer matrix is highly dependent on the degree of dispersion achieved during mixing[9]; hence sometimes surface modification of the nanoclays is required in order to increase their compatibility.

As seen in Figure 1(a), the presence of small intercalated structures with a large aspect ratio (tactoids) in the PHBV–C30B is observed. Nevertheless, the nanocomposite shows a good dispersion of the montmorillonite platelets, also indicating that a high degree of delamination of the clay during melt processing was achieved.

The TEM micrograph of the PHBV–HNT sample [Figure 1(b)] shows the presence of isolated nanotubes. In this figure, it is possible to identify a parallel-oriented nanotube showing the internal structure of the halloysite, which can be described as a hollow tubular morphology produced by the stacking of the clay mineral layers. From the TEM pictures, the dimensions of the halloysite tubes could be estimated: a length below 1 µm and external and internal nanotube diameters of 70 and 25 nm, respectively. The good dispersion of the unmodified halloysite can be adscribed to its structure; i.e., the surface of HNTs comprised siloxane and hydroxyl groups, which gives halloysites potential for the formation of hydrogen bonds and hence improves the dispersion in some polymer matrixes without any chemical modification, especially when compared to other two-dimensional nanoclay fillers such as montmorillonites.[37,38]

SEM micrographs of PHBV nanocomposites with and without TNPP are presented in Figure 2. In the case of montmorillonite

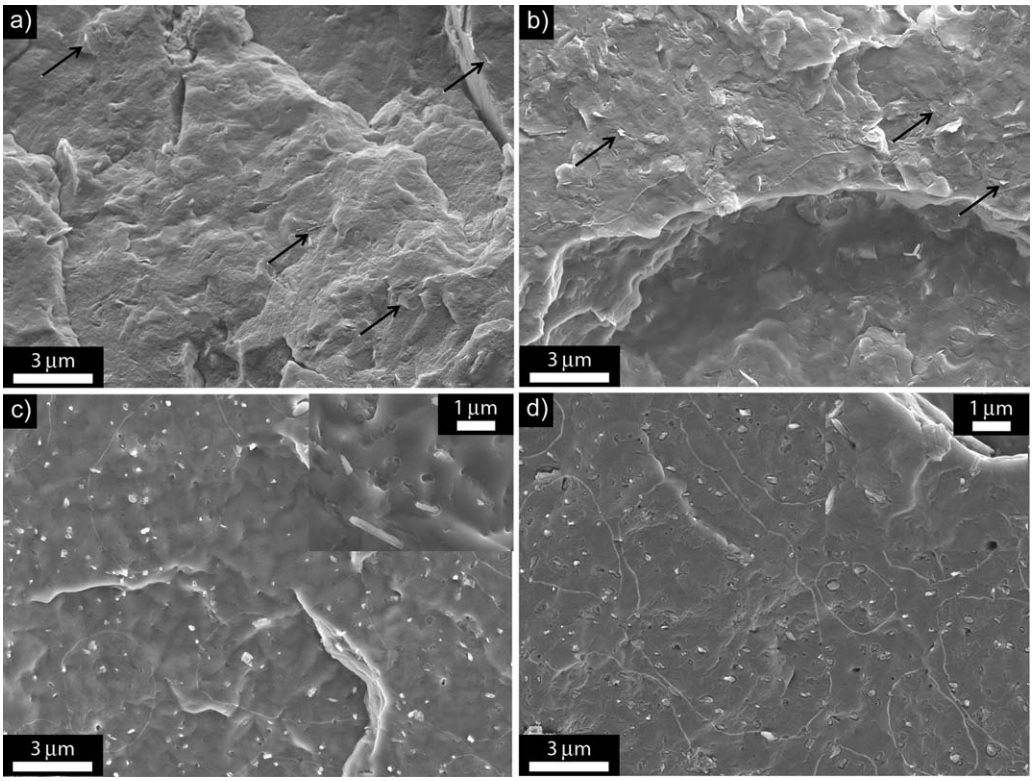

Figure 2. SEM images of the fracture surface of (a) PHBV–C30B, (b) PHBV–C30B–TNPP, (c) PHBV–HNT, and (d) PHBV–HNT–TNPP.

nanocomposites [Figure 2(a,b)], a strong adhesion between the clay and the polymer matrix can be deduced from the look of the platelets, covered with the polymer matrix. In these figures, it is possible to observe the presence of individual platelets (indicated with an arrow), as well as a good dispersion, in agreement with the TEM micrographs. Hence, it can be inferred that an effective mixing has been achieved.

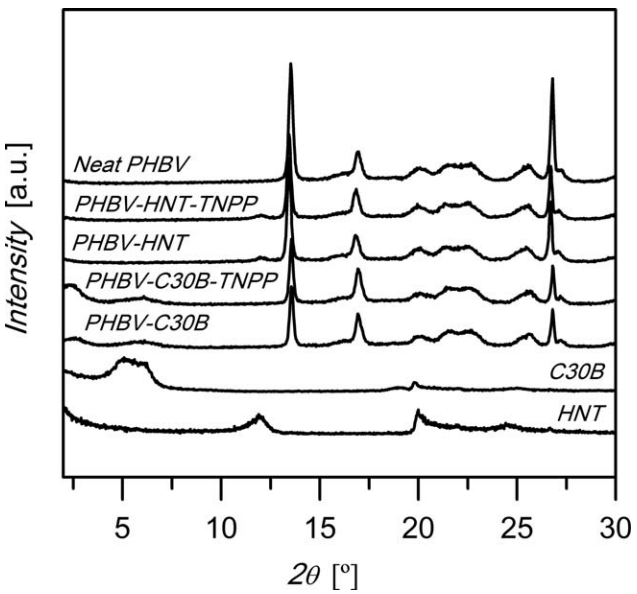

Figure 3. WAXS pattern of neat PHBV, PHBV–C30B, and PHBV–HNT nanocomposites.

The SEM micrographs of PHBV–HNT nanocomposites present a uniform dispersion of the halloysite nanotubes in both cases (with and without TNPP), shown as white dots in Figure 2(c,d). These micrographs are in agreement with TEM observations. However, different surface interaction between the halloysite and the PHBV can be observed depending on the presence of the chain extender. The sample without TNPP exhibits a good degree of adhesion of the polymer matrix on the nanoclay surface. The sample containing TNPP shows a slight detachment of the nanotubes from the polymer matrix. A possible explanation for this behavior is that the TNPP is partially absorbed on the surface of the nanotubes, thus leading to a decrease in the interaction between the nanoclay surface and the polymer matrix.

The WAXS diffractograms of the clays and PHBV nanocomposites are shown in Figure 3. The PHBV diffractogram presents three main peaks at 2θ values of 13, 17, and 26. The first two peaks can be associated with the (020) and (110) reflections of the orthorhombic lattice of the PHBV, respectively. The most intense peak at $2\theta = 26$ corresponds to the (002) reflexion of the boron nitride, which is present as a nucleating agent in the commercial grade used in this work. No noticeable difference in the peak positions and relative intensities can be observed when the clays or the TNPP are introduced; therefore, it can be concluded that the crystalline form of the PHBV is not affected by the addition of these nanoclays or the chain extender.

The diffraction pattern of C30B exhibits a peak at $2\theta = 5°$, corresponding to a basal spacing (001) of 1.76 nm according to the Bragg equation. The PHBV–C30B diffractogram shows the peak

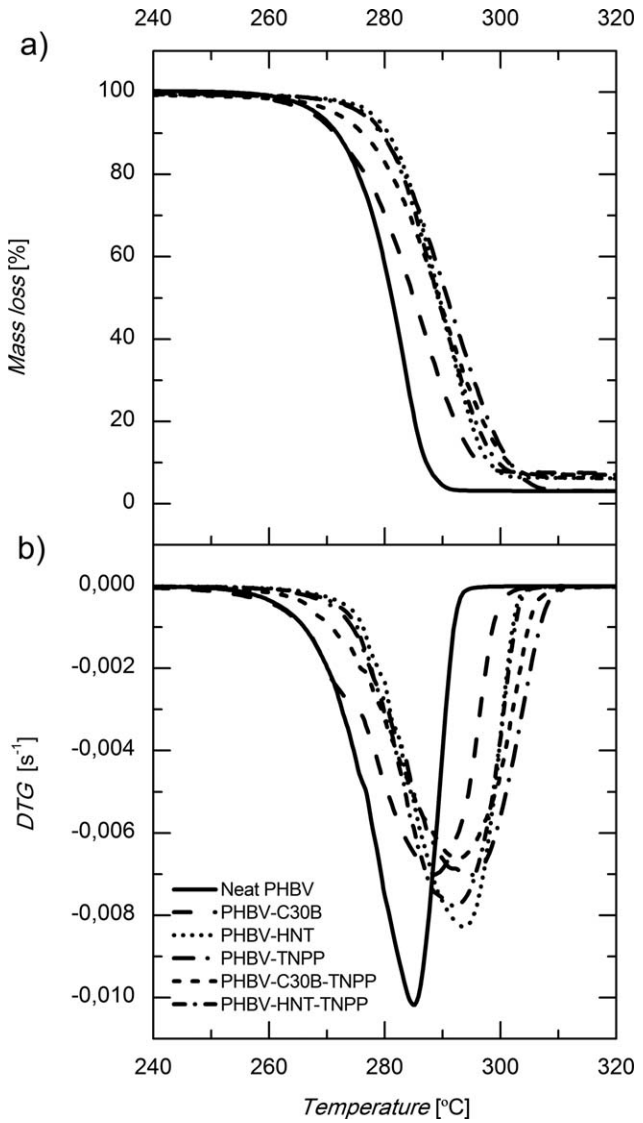

Figure 4. TGA and DTG curves of PHBV and PHBV/clay nanocomposites with and without chain extender.

associated with the basal reflection of the C30B, which suggests that fully exfoliated morphology has not been achieved. However, a shift toward lower angles is observed, indicating an increase in the interlayer gallery, associated with a predominantly intercalated morphology.

Regarding the samples containing HNTs, it is possible to observe the most intense diffraction peak of HNT (001) at $2\theta = 11.95°$ (corresponding to a basal spacing of 0.74 nm). No changes were observed in the shape or position of this peak in the PHBV–HNT nanocomposites. This result indicates that after blending no changes occur in the tubular structure of the primary particles of halloysite. The addition of chain extender does not affect either the crystalline structure of PHBV or the interlayer distance of the clay.

Thermal Characterization

TGA experiments were carried out to investigate the effect of the addition of clay and chain extenders on the thermal stability of PHBV. Figure 4 plots the mass loss and the DTG versus temperature for the neat PHBV and PHBV nanocomposites, while Table I summarizes the values of $T_{5\%}$ and T_d for all the samples studied.

Table I. DSC and TGA Data of the Samples Studied (González-Ausejo *et al.*)

	TGA parameters			DSC parameters		
	T_c (°C)	T_m (°C)	ΔH_c (J/g)	X_c (%)	$T_{5\%}$ (°C)	T_d (°C)
Neat PHBV	115	169	96	66	268	285
PHBV-C30B	115	164	96	66	267	288
PHBV-HNT	115	166	98	67	277	294
PHBV-TNPP	113	166	97	66	276	295
PHBV-C30B-TNPP	114	165	100	68	272	293
PHBV-HNT-TNPP	115	169	97	66	277	292

The thermal degradation of neat PHBV consists of a single weight loss step between 240 and 320°C (Figure 4), according to the random chain scission reaction.[39] The maximum rate of mass loss takes place at 285°C and $T_{5\%}$ (the temperature at which the mass loss is 5%) is of 268°C. Some differences in the thermal degradation of PHBV are observed with the incorporation of the clays.

Once the degradation has begun, the reaction rate clearly decreases with respect to the pure polymer, showing a higher T_d with respect PHBV, from 285 to 288 and 294°C for C30B and HNT, respectively. This behavior can be explained by the fact that the clays, together with the solid degradation products, generate a dense coating that hinders the development of further degradation by opposing a strong mass transport resistance to the volatile agents involved in the reaction, resulting in a decrease of the degradation kinetics.[40] These results are in agreement with the work reported by Bittmann *et al.* and Bruzaud *et al.* in which different nanoclays (non modified montmorillonite, bentonite and Cloisite® 15A) showed similar trends in TGA.

With respect to the presence of HNT in the PHBV matrix, it also increases the thermal stability of PHBV, with a rise in $T_{5\%}$ from 268 to 277°C. The sample containing C30B exhibits a degradation onset similar to that of the neat PHBV, as derived from the $T_{5\%}$. In other works, it has been reported a decrease on the $T_{5\%}$ for PHBV/C30B composites.[41–44] This behavior is generally attributed to the clay modifiers that may have a catalytic action in the degradation of PHBV.[14] In our case, the opposed phenomena of stabilizing by the clays[45,46] compensates the catalytic degradation generated by the organomodifier,[11–13] resulting in no significant variation on the $T_{5\%}$. Additionally, it has been suggested that the water adsorbed to the clays may contribute to accelerate the degradation rate in clay/PHBV composites, hindering the thermal stabilizing effect of the clays.[41] The thermal history and severity of processing conditions, especially with clays, may have also an influence on the degradation kinetics of the samples.[47]

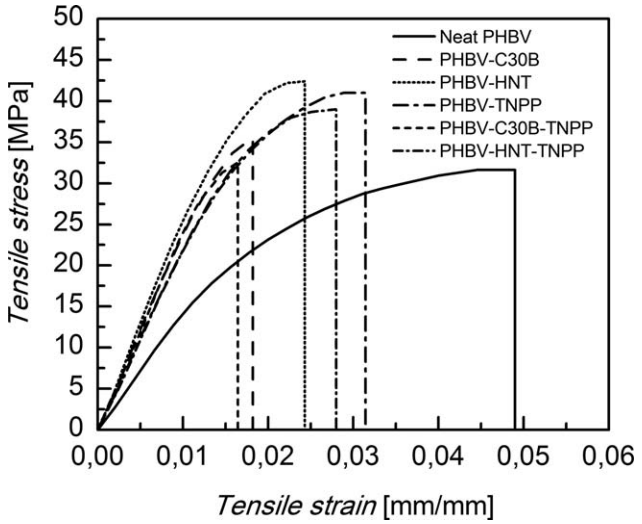

Figure 5. Stress–strain curves of PHBV and PHBV/clay nanocomposites with and without chain extender.

The effect of the addition of TNPP to both neat PHBV and the nanocomposites on the thermal degradation behavior can be seen in Figure 5. As expected, the presence of the chain extender improves the thermal stability of PHBV, as derived from the increases of $T_{5\%}$ and T_d by 8 and 10°C, respectively. This issue is of special relevance since during food packaging operations, there are many thermic cycles (film processing, stretching, thermoforming, hot sealing, etc.) where some local thermal degradation can occur, being the products of such degradation susceptible to migrate toward the content of the package.[48] This trend is in concordance with the literature where the TNPP has been used as chain extender in other matrices.[25–27]

The addition of TNPP to the sample containing C30B clay revealed a shift of the curve toward higher temperatures, thus showing an increase of ca. 5°C in both $T_{5\%}$ and T_d with respect to that without the chain extender. These results would indicate that the addition of TNPP to PHBV/clay nanocomposites may improve their thermal resistance. The PHBV–HNT–TNPP sample does not show relevant changes in thermal degradation when compared with that without the chain extender. This lack of a synergetic effect between the TNPP and the halloysite could be explained by the fact that, as inferred from the SEM analysis, the TNPP is partially adsorbed over the surface of the clay, thus decreasing the chain extender activity.

DSC experiments were conducted in order to evaluate the influence of the addition of the nanoclays and chain extender on the crystallization characteristics of PHBV. Table I summarizes the crystallization and melting temperatures, crystallization enthalpy, and degree of crystallinity of all the samples studied in this work.

After analyzing the resulting DSC parameters, it can be appreciated that the crystallization temperature (T_c) of PHBV was not significantly modified when the nanoclays were incorporated. The degree of crystallinity (X_c) also remained similar, at around 66%, in agreement with other works and a similar processing history.[32,49] During the second heating scan, it could be observed that the peak melting temperature (T_m) decreased by about 5°C with C30B and 3°C with HNT. These results suggest that nanoclays make the formation of thick lamella more difficult than neat PHBV, being more pronounced in the case of C30B.

When TNPP was added to PHBV, a small decrease on T_m is detected, pointing to some reduction in lamellar thickness; but when it is combined with C30B or HNT, the T_m increases slightly with respect to the composites without TNPP. In any case, it is considered that the variations in T_c, X_c, and T_m shown are not of great significance, indicating that 1 wt % of TNPP has little interference with the crystallization processes of PHBV.

Mechanical Properties

Tensile tests to rupture were conducted on hot-pressed films for all the samples studied. Figure 5 shows the strain–stress representative curves for the neat PHBV and PHBV nanocomposites. From the stress–strain curves were obtained the average values of Young's modulus, tensile strength, and elongation at break of PHBV with the addition of clays and TNPP, these values are shown in Figure 6. The Young's modulus of PHBV showed significant increases of 69 and 80% with the addition of 5 wt % C30B and HNT, respectively. Regarding the tensile strength, increases of 12 and 34% were detected with the addition of both C30B and HNT. This enhancement in stiffness and tensile strength of PHBV/clay nanocomposites was at the expense of a significant reduction in the elongation at break [Figure 6(c)]. In this sense, drops of 63 and 50% in the elongation at break can be observed with the addition of 5 wt % C30B and HNTs, respectively. Altogether these results show a clear reinforcing effect of the nanoclays on the PHBV matrix. The higher reinforcement observed for the samples containing HNTs as compared to the ones with montmorillonite platelets can be explained by the higher stiffness and length-to-diameter aspect ratio of the nanotubes. This behavior has also been reported in other works.[11,38,45,50]

The addition of TNPP to the neat PHBV resulted in increases in the Young's modulus (44%) and the tensile strength (30%), similar to those obtained by the addition of nanoclays. Some studies with PCL and PLA showed that the increase in the Young's modulus and tensile strength with the addition of chain extenders could be ascribed to the increased molecular weight, together with the formation of a long-chain branching structure.[20,51,52] The strain at break of PHBV containing the chain extender decreases compared to that of the original polymer. This can be explained by the fact that the increased density of entanglements of the polymer structure with the long-chain branching hinders the slipping of the polymer chains.[20,53,54]

Regarding the combined effect of the nanoclays with the TNPP on the mechanical properties of PHBV, surprisingly, no relevant changes were observed when TNPP was added to PHBV–C30B nanocomposites. However, an increase in elongation at break and a decreased Young's modulus and tensile strength with respect to the PHBV–HNT nanocomposite were observed. Such different behavior could be attributed to the effect of partial absorption of TNPP on the clay surface discussed previously on the morphological and thermal stability analysis. This can also

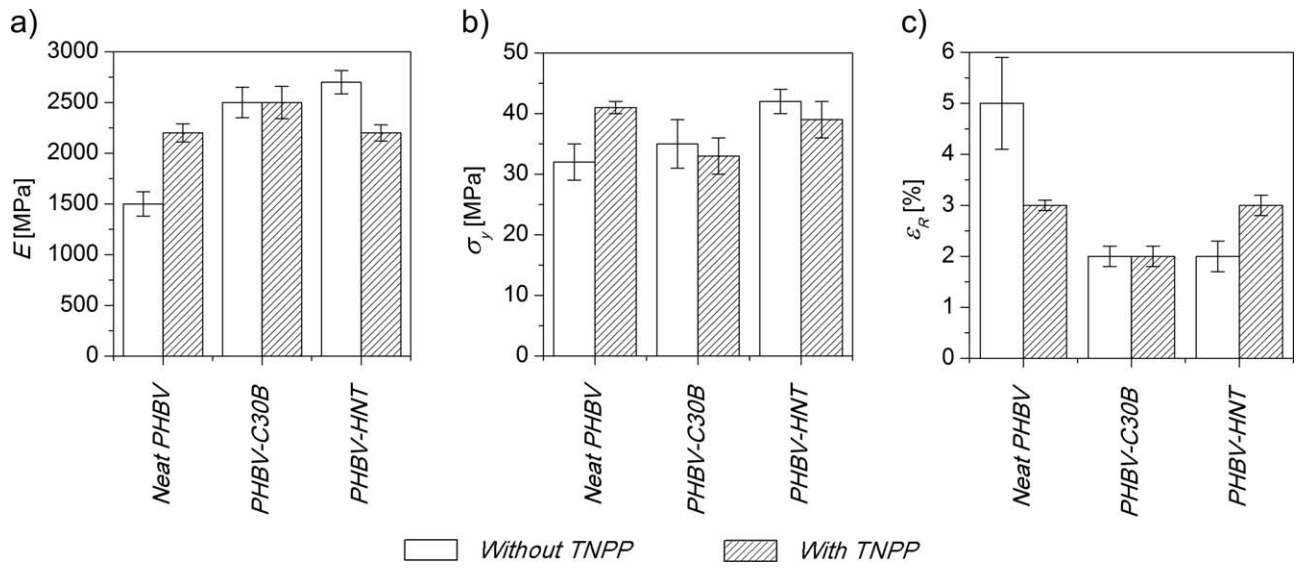

Figure 6. Young's modulus (E), tensile strength (σ_y), and elongation at break (ε_R) of PHBV/clay nanocomposites with and without chain extender.

explain why mechanical properties of the PHBV/HNT/TNPP nanocomposites are similar to those of PHBV/TNPP, since the reinforcement of the HNT is limited by the partial absorption of the TNPP on its surface. These results suggest that the properties of PHBV/HNT nanocomposites could be improved by modifying the mixing procedures, in order to minimize the absorption of TNPP on the active surface of HNT.

The improvement on mechanical properties opens up the possibility to reduce thickness in food packaging products, thus decreasing the overall costs while preserving the other characteristics of the package. It is worthwhile to recall that this type of industry uses large amounts of raw material and a reduction of 5–10% in volume may have a huge impact of the final economic and environmental balance of the package.

CONCLUSIONS

PHBV nanocomposites with two different clays (Cloisite® 30B and halloysite nanotubes) and a chain extender (TNPP) were successfully obtained by melt blending. Favorable morphologies were achieved during processing for both nanoadditives (i.e., predominantly intercalated morphology in the PHBV–C30B and good distribution of halloysite nanotubes within the polymer matrix) as derived from TEM, SEM, and WAXS experiments.

The properties of such compounds are characterized by an increase in the thermal stability of PHBV through incorporation of TNPP as a chain extender or HNT. The addition of C30B only improves the thermal stability by decreasing the degradation rate. The crystallization temperature and overall crystallinity of the compounds was not altered by the addition of clays or TNPP.

Regarding the mechanical properties, the nanocomposites prepared with C30B and HNT revealed a reinforced behavior when compared to the neat PHBV, with higher stiffness and tensile strength and a decreased elongation at break. However, no relevant changes were observed when TNPP was added to PHBV nanocomposites.

ACKNOWLEDGMENTS

Financial support for this research from Ministerio de Economía y Competitividad (project MAT2012–38947-C02-01), Generalitat Valenciana (GV/2014/123), and Pla de Promoció de la Investigació de la Universitat Jaume I (PREDOC/2012/32) is gratefully acknowledged. The authors are also grateful to Raquel Oliver and José Ortega for experimental support.

REFERENCES

1. Lenz, R. W.; Marchessault, R. H. *Biomacromolecules* **2005**, *6*, 1.
2. Chea, V.; Angellier-Coussy, H.; Peyron, S.; Kemmer, D.; Gontard, N. *J. Appl. Polym. Sci.* **2015**, to appear.
3. Bucci, D. Z.; Tavares, L. B. B.; Sell, I. *Polym. Test.* **2005**, *24*, 564.
4. Cava, D.; Gimenez, E.; Gavara, R.; Lagaron, J. M. *J. Plast. Film Sheeting* **2006**, *22*, 265.
5. Lagaron, J. M.; Lopez-Rubio, A. *Trends Food Sci. Technol.* **2011**, *22*, 611.
6. Rhim, J.-W.; Park, H.-M.; Ha, C.-S. *Prog. Polym. Sci.* **2013**, *38*, 1629.
7. Lagarón, J. M.; Cabedo, L.; Cava, D.; Feijoo, J. L.; Gavara, R.; Gimenez, E. *Food Addit. Contam.* **2005**, *22*, 994.
8. Bordes, P.; Pollet, E.; Averous, L. *Prog. Polym. Sci.* **2009**, *34*, 125.
9. Sanchez-Garcia, M. D.; Lagaron, J. M. *J. Appl. Polym. Sci.* **2010**, *118*, 188.
10. Reddy, M. M.; Vivekanandhan, S.; Misra, M.; Bhatia, S. K.; Mohanty, A. K. *Prog. Polym. Sci.* **2013**, *38*, 1653.

11. Carli, L. N.; Crespo, J. S.; Mauler, R. S. *Compos. Part A: Appl. Sci. Manuf.* **2011**, *42*, 1601.
12. Cabedo, L.; Plackett, D.; Giménez, E.; Lagarón, J. M. *J. Appl. Polym. Sci.* **2009**, *112*, 3669.
13. Bordes, P.; Hablot, E.; Pollet, E.; Avérous, L. *Polym. Degrad. Stab.* **2009**, *94*, 789.
14. Bellucci, F.; Camino, G.; Frache, A.; Sarra, A. *Polym. Degrad. Stab.* **2007**, *92*, 425.
15. Hablot, E.; Bordes, P.; Pollet, E.; Avérous, L. *Polym. Degrad. Stab.* **2008**, *93*, 413.
16. Shi, Y.-F.; Tian, Z.; Zhang, Y.; Shen, H.-B.; Jia, N.-Q. *Nanoscale Res. Lett.* **2011**, *6*, 608.
17. Guimarães, L.; Enyashin, A. N.; Seifert, G.; Duarte, H. A. *J. Phys. Chem. C* **2010**, *114*, 11358.
18. Liu, Q.-S.; Zhu, M.-F.; Wu, W.-H.; Qin, Z.-Y. *Polym. Degrad. Stab.* **2009**, *94*, 18.
19. Najafi, N.; Heuzey, M. C.; Carreau, P. J. *Polym. Eng. Sci.* **2013**, *53*, 1053.
20. Najafi, N.; Heuzey, M. C.; Carreau, P. J.; Wood-Adams, P. M. *Polym. Degrad. Stab.* **2012**, *97*, 554.
21. Najafi, N.; Heuzey, M. C.; Carreau, P. J. *Compos. Sci. Technol.* **2012**, *72*, 608.
22. Al-Itry, R.; Lamnawar, K.; Maazouz, A. *Polym. Degrad. Stab.* **2012**, *97*, 1898.
23. Meng, Q.; Heuzey, M.-C.; Carreau, P. J. *Polym. Degrad. Stab.* **2012**, *97*, 2010.
24. Rytlewski, P.; Żenkiewicz, M.; Malinowski, R. *Int. Polym. Process.* **2011**, *26*, 580.
25. Burlet, J.; Heuzey, M. C.; Dubois, C.; Wood-Adams, P.; Brisson, J. Annu. Tech. Conf. - ANTEC, Conf. Proc. **2005**, *3*, 281.
26. Cicero, J. A.; Dorgan, J. R.; Dec, S. F.; Knauss, D. M. *Polym. Degrad. Stab.* **2002**, *78*, 95.
27. Lehermeier, H. J.; Dorgan, J. R. *Polym. Eng. Sci.* **2001**, *41*, 2172.
28. D'Haene, P.; Remsen, E. E.; Asrar, J. *Macromolecules* **1999**, *32*, 5229.
29. Bikiaris, D.; Karayannidis, G. *J. Polym. Sci. Part A Polym. Chem.* **1996**, *34*, 1337.
30. D'Haene, P.; Remsen, E. E.; Asrar, J. *Macromolecules* **1999**, *32*, 5229.
31. Fei, B.; Chen, C.; Chen, S.; Peng, S.; Zhuang, Y.; An, Y.; Dong, L. *Polym. Int.* **2004**, *53*, 937.
32. Duangphet, S.; Szegda, D.; Song, J.; Tarverdi, K. *J. Polym. Environ.* **2013**, *22*, 1.
33. Fensterheim, R. J. In Society of Plastics Engineers - International Polyolefins Conference - FLEXPACKCON 2008; **2008**; Vol. 2, p 643.
34. Savenkova, L.; Gercberga, Z.; Bibers, I.; Kalnin, M. *Process Biochem.* **2000**, *36*, 445.
35. Heo, K.; Yoon, J.; Jin, K.; Jin, S. *J. Phys. Chem.* **2008**, *112*, 4571.
36. Alata, H.; Aoyama, T.; Inoue, Y. *Macromolecules* **2007**, *40*, 4546.
37. Joussein, E.; Petit, S.; Churchman, J.; Theng, B.; Righi, D.; Delvaux, B. *Clay Miner.* **2005**, *40*, 383.
38. Rawtani, D.; Agrawal, Y. *Rev. Adv. Mater. Sci.* **2012**, *30*, 282.
39. Grassie, N.; Murray, E. J.; Holmes, P. A. *Polym. Degrad. Stab.* **1984**, *6*, 127.
40. Du, M.; Guo, B.; Jia, D. *Eur. Polym. J.* **2006**, *42*, 1362.
41. Carli, L. N.; Crespo, J. S.; Mauler, R. S. *Compos. Part A: Appl. Sci. Manuf.* **2011**, *42*, 1601.
42. Carli, L. N.; Daitx, T. S.; Soares, G. V.; Crespo, J. S.; Mauler, R. S. *Appl. Clay Sci.* **2014**, *87*, 311.
43. Wang, S.; Song, C.; Chen, G.; Guo, T.; Liu, J.; Zhang, B.; Takeuchi, S. *Polym. Degrad. Stab.* **2005**, *87*, 69.
44. Bordes, P.; Pollet, E.; Bourbigot, S.; Avérous, L. *Macromol. Chem. Phys.* **2008**, *209*, 1473.
45. Javadi, A.; Srithep, Y.; Pilla, S. *Polym. Eng. Sci.* **2011**, *51*, 1815.
46. Bruzaud, S.; Bourmaud, A. *Polym. Test.* **2007**, *26*, 652.
47. Zaverl, M.; Seydibeyoğlu, M. Ö.; Misra, M.; Mohanty, A. *J. Appl. Polym. Sci.* **2012**, *125*, E324.
48. Incarnato, L.; Di Maio, L.; Acierno, D.; Denaro, M.; Arrivabene, L. *Food Addit. Contam.* **1998**, *15*, 195.
49. Crétois, R.; Follain, N.; Dargent, E.; Soulestin, J.; Bourbigot, S.; Marais, S.; Lebrun, L. *J. Memb. Sci.* **2014**, *467*, 56.
50. Russo, P.; Vetrano, B.; Acierno, D.; Mauro, M. *Polym. Compos.* **2013**, *34*, 1460.
51. Liu, J.; Lou, L.; Yu, W.; Liao, R.; Li, R.; Zhou, C. *Polymer (Guildf)* **2010**, *51*, 5186.
52. Grosvenor, M. *Int. J. Pharm.* **1996**, *135*, 103.
53. Kennedy, M. A.; Peacock, A. J.; Mandelkern, L. *Macromolecules* **1994**, *27*, 5297.
54. Lin, G.; Shih, H. *Polym. Eng. Sci.* **2002**, *42*, 2213.